

Advanced Higher Physics Project Report

On the Properties of Capacitive and Inductive AC Circuits

Andrew Robertson

Abstract

The three foundational circuit elements, resistors (R), inductors (L), and capacitors (C), are ubiquitous in electronic circuits. The combined properties of these components are an interesting area of discussion and can offer some great insight on why modern technology is entirely dependent on these elements. In this report, the characteristics of multiple configurations of the R, L, and C components under alternating current (AC) systems have been investigated. The relationships between capacitive reactance and frequency ($X_C \propto 1/f$), and inductive reactance and frequency ($X_L \propto f$) have been attempted to be shown through measurement of voltage at different frequencies. Resonance in series and parallel RLC circuits is observed, where voltage either spikes or dips at specific frequency values f_0 . The transient responses of series RLC circuits with differing resistances are justified as damped harmonic oscillators, with investigations into under-, critically-, and over-damped systems. Throughout, the phase relationships between the voltages across different components are also explored, though weakly explained.

Contents

I Equipment List	3
II Oscilloscope Remarks	3
III GitHub Repository	3
1 Isolated RC and RL Circuits	4
1.1 Underlying Physics	4
1.2 Experiment Description	5
1.3 Results	7
1.4 Discussions and Conclusions	11
1.4.1 Series RC Circuit	11
1.4.2 Series RL Circuit	17
1.4.3 Resonance Inquiry	21
2 Series and Parallel RLC Circuits	23
2.1 Underlying Physics	23
2.2 Experiment Description	24
2.3 Results	26
2.4 Discussions and Conclusions	29
2.4.1 Series RLC Circuit	29
2.4.2 Parallel RLC Circuit	32
3 Series RLC Transient Responses	35
3.1 Underlying Physics	35
3.2 Experiment Description	36
3.3 Results	38
3.4 Discussions and Conclusions	40
3.4.1 Underdamped Circuits	40
3.4.2 Critically-Damped and Overdamped Circuits	42
4 Evaluation of	43
4.1 Procedures	43
4.2 Project	44
References	46

I Equipment List

Since all experiments require similar equipment, the equipment list will be stated here to avoid repetition. Specific values for circuit components will be clarified in experiment descriptions.

- Digital oscilloscope
 - Signal generator
 - Dual-trace oscilloscope
- Resistors
- Inductors
- Capacitors
- BNC to crocodile clip test lead
- 2 oscilloscope probes
- Terminal blocks

II Oscilloscope Remarks

The digital oscilloscope used for this report is the Hantek DSO2000 Series Digital Storage Oscilloscope with an internal impedance of $50\Omega \pm 1\%$ [1, p. 66]. This oscilloscope includes both a signal generator and dual-trace oscilloscope screen. All measurements made come from the *measurement* and *cursor* functions of the oscilloscope. The inconsistency across the precision of measurements and reading uncertainties are due to variations in the combination of y-gain and time-base values.

III GitHub Repository

Details on how the data used in this project was post-processed and analysed can be found on my GitHub repository [2]. Here, all figures, tables and spreadsheets are found. As well as Jupyter notebook files displaying the code used to create the graphs. There is also an online PDF version of this report there.

1 Isolated RC and RL Circuits

Aims: Verify $X_C = \frac{1}{2\pi fC}$ and $X_L = 2\pi fL$. Analyse voltage phase difference between components at different AC frequencies. Investigate whether resonance frequency f_0 can be derived from separate RC and RL circuits.

1.1 Underlying Physics

The capacitor, named as such for its *capacity* to store electric charge in its own electric field. In its simplest form, the capacitor is realised with two parallel conductive plates (acting as anode and cathode) separated by a dielectric insulator [3, p. 44]. This component, when subject to direct current (DC) driven by a power source, results in a surplus of electrons on the cathode side and deficit on the anode side. This creates a potential difference across the capacitor plates, with the charge stored in the capacitor being proportional to the voltage across it. In this case, the constant of proportionality between the two values is the capacitance C of the capacitor, measured in Farads F.

The interest of capacitors in this investigation is not their properties under DC, but instead AC. The main distinction between the two is that current that periodically reverses polarity (AC) is not blocked by the capacitor. In the DC case, after a period of charging, the current across the capacitor drops to zero. Whereas, in the AC case, the capacitor still charges up to a certain voltage (depending on the frequency of the supply) but will discharge when the supply current passes zero and then recharge in the opposite direction when the current flips direction [3, pp. 52–53]. It is still worth mentioning that no current physically passes through the capacitor, despite it appearing so. Charges only redistribute themselves between the plates.

However, capacitors still provide an opposition to the current in AC circuits, called capacitive reactance (X_C). This is similar to the resistance provided by a resistor but differs mainly in that X_C is frequency dependent. Experimentally showing the formula $X_C = \frac{1}{2\pi fC}$ [4, p. 201] is the focus of the first experiment.

The next component under investigation, aside from the resistor, is the inductor. Getting its name from its ability to store energy in a magnetic field by self-*inducing* an emf across its ends [4, p. 194]. Current flowing through a wire produces a magnetic field, when the wire is wound into a coil, the strength of the produced magnetic field increases – this is an inductor. The emf induced is proportional, but in opposition, to the rate of change

of current passing through the coil. This is the result of Faraday's and Lenz's laws. The inductance L of the inductor is the constant of proportionality, with units Henrys H.

Faraday's Law: "the greater the rate at which the magnetic field changes..., the greater the induced voltage".

Lenz's law: "the induced voltage (and current) always opposes what causes it". [3, p. 63]

These laws apply to both DC and AC systems. For AC systems with a high frequency, a larger emf is expected, therefore voltage should increase with frequency (from Faraday's law). Like capacitors, inductors also have *inductive* reactance X_L which opposes AC (from Lenz's law). The second part of the first experiment will investigate this, through showing $X_L = 2\pi fL$ [4, p. 200].

1.2 Experiment Description

A resistor ($39\Omega \pm 5\%$) and capacitor ($1000\mu F \pm 20\%$) were connected in series by a terminal block. This circuit was then hooked up to the signal generator (plugged in), with the resistor on the signal side. Channel 1 of the oscilloscope probed across the resistor, and channel 2 across the capacitor. Only one ground probe needed to be connected, as oscilloscopes have an internal common ground.

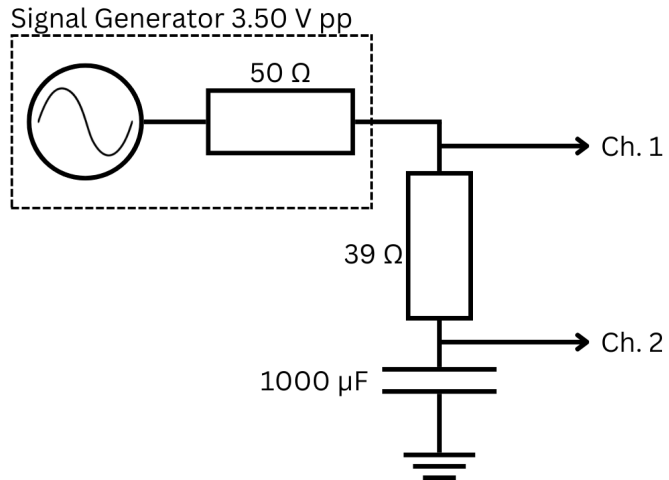
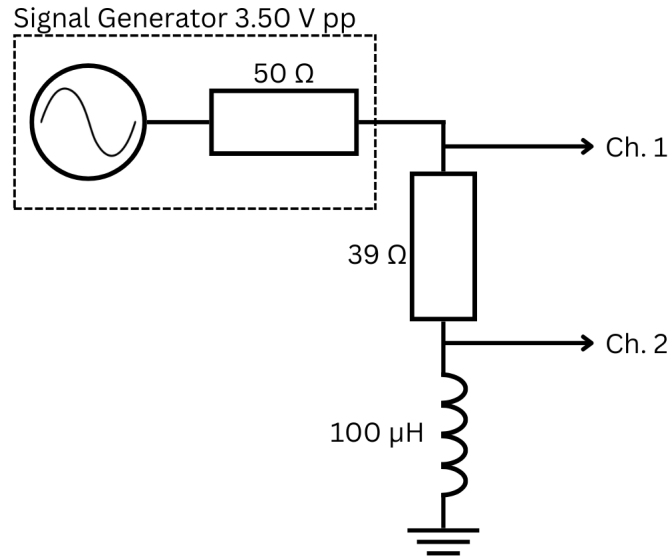


Figure 1: Series RC circuit diagram.

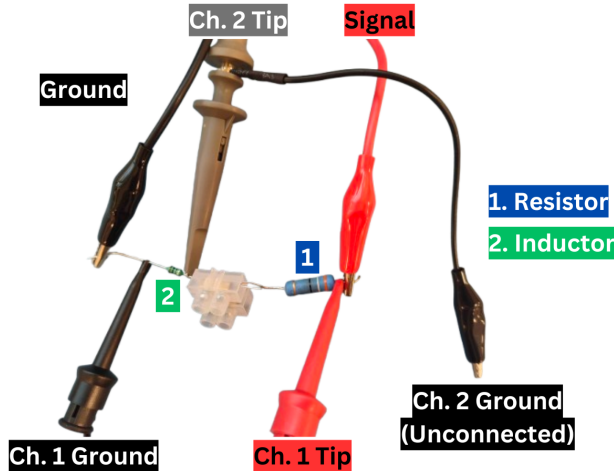
After setting up the circuit, the signal source was set to repeating sinusoidal (to create an AC sine waveform). The desired frequency to be measured for was then set. On the oscilloscope screen, peak-to-peak voltages for both traces were measured, as well as the time difference between traces with respect to the channel 2 trace. This is to calculate

how the voltage phase difference varies with frequency.¹ The reading uncertainty was recorded for every measurement.

All measurements were repeated, for a total of 5 individual values per frequency. For this experiment, a total of 40 frequencies were measured for in logarithmic increments, see Tables 1 through 4 for frequency values used. After the RC circuit measurements were collected, the capacitor was swapped out for an inductor ($100 \mu\text{H} \pm 5\%$) and the above steps were repeated.



(a) Circuit diagram with component values.



(b) Circuit realisation and connections.

Figure 2: Series RL circuit diagrams.

¹Important note: not all oscilloscopes will have these functionalities.

1.4 Discussions and Conclusions

1.4.1 Series RC Circuit

From the V_C and V_R columns of Tables 1 and 2, Figures 3 and 4 can be plotted. The vertical error bars are the absolute uncertainties calculated from the random, reading and calibration uncertainties for each measurement. The 20% calibration uncertainty for V_C comes from the capacitor, and the 5% for V_R from the resistor's uncertainty. The horizontal error bars (squint and you'll see them) are the digital reading uncertainties of the signal generator's frequency.

Although the tables above show peak-to-peak voltages, voltage has been converted to rms for the graphs. This has been done by dividing the mean voltages from the tables by $2\sqrt{2}$. The conversion has been done for the majority of graphs in this report.

Most graphs are also semi-log, with logarithmic x-axis. This has been done to better suit the scaling of the measurements, which were intentionally logarithmic.

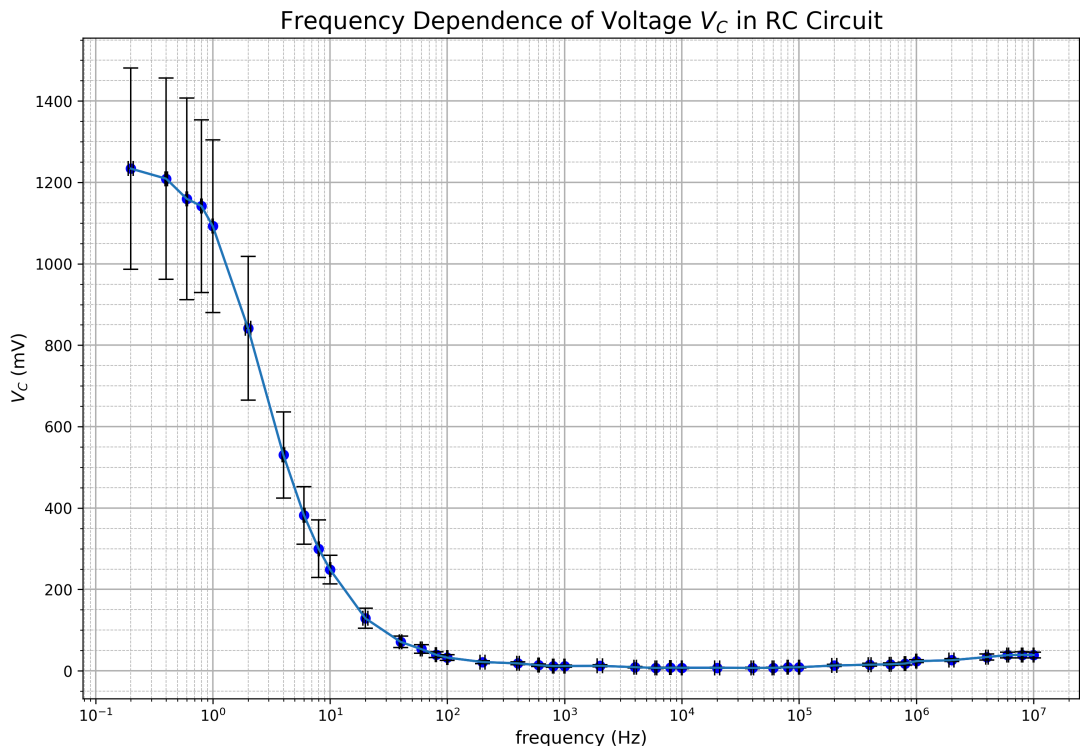


Figure 3: V_C against frequency for series RC circuit.

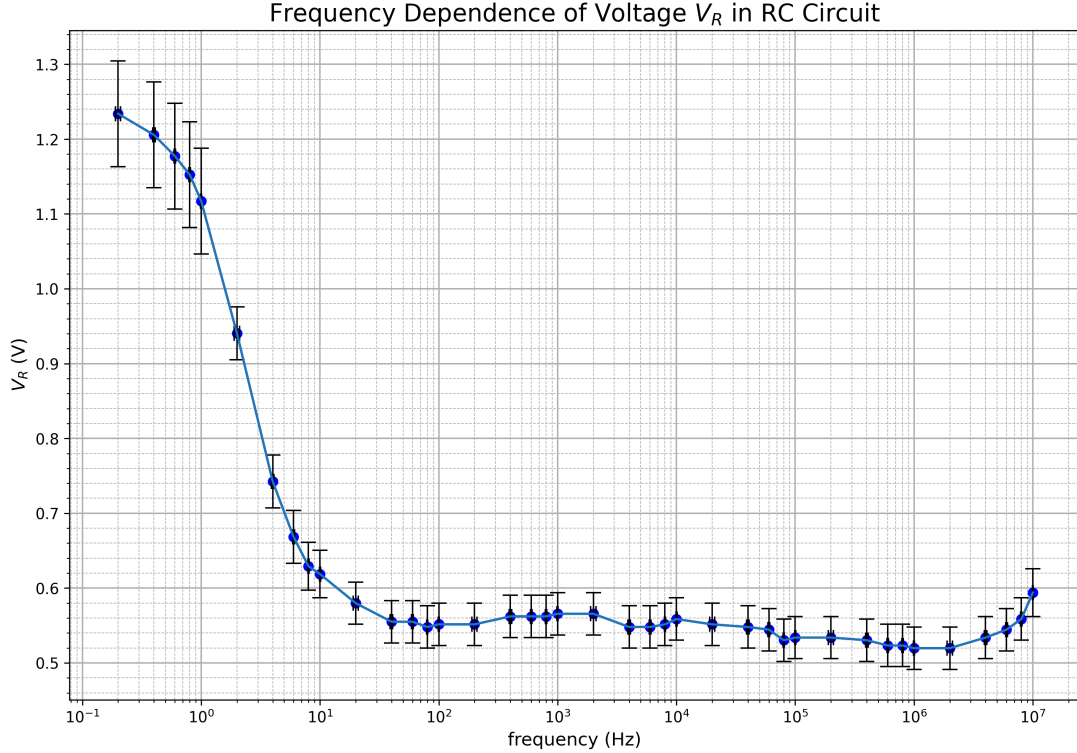


Figure 4: V_R against frequency for series RC circuit.

From Figures 3 and 4, it is clear that voltage, generally, decreases with frequency. Both graphs show voltage levelling out after 100 Hz (approx.). With the key distinction being that V_C drops to below 50 mV_{rms} whereas V_R drops to around 550 mV_{rms}.

However, neither of these graphs can serve as verification to the relation $X_C = \frac{1}{2\pi f C}$ or even $X_C \propto 1/f$. Since no current measurement was made (due to the oscilloscope not having a current measurement function, and available ammeters being unsuitable for AC) X_C cannot be calculated by V_C/I directly. Instead, current can be calculated from impedance relations [5].

$$V_t = I|Z| \quad (1)$$

$$= I\sqrt{R^2 + X_C^2} \quad (2)$$

Where V_t is the total circuit voltage (1.24 V_{rms}), and R is the total circuit resistance ($50\Omega + 39\Omega = 89\Omega$). Rearranging for I gives:

$$I = \frac{V_t}{\sqrt{R^2 + X_C^2}} \quad (3)$$

Substituting I into $V_C = IX_C$:

$$V_C = \frac{V_t X_C}{\sqrt{R^2 + X_C^2}} \quad (4)$$

All values in Equation 4 are measurements available from the experiment, so X_C can now be solved:

$$X_C = \frac{V_C R}{\sqrt{V_t^2 - V_C^2}} \quad (5)$$

All values in Equation 5 have known uncertainties, except for V_t , so the absolute uncertainty in X_C , ΔX_C , needs to be calculated. Working outwards (from the uncertainty in the radical, to denominator, then to fraction) gives:

$$\Delta X_c = X_C \sqrt{\left(\frac{\Delta V_C}{V_C}\right)^2 + \left(\frac{\Delta R}{R}\right)^2 + \left(\frac{\Delta \sqrt{V_t^2 - V_C^2}}{\sqrt{V_t^2 - V_C^2}}\right)^2} \quad (6)$$

$$= X_C \sqrt{2 \left(\frac{\Delta V_C}{V_C}\right)^2 + \left(\frac{\Delta R}{R}\right)^2} \quad (7)$$

Note: $\Delta R = R\sqrt{0.01^2 + 0.05^2}$, for the calibration uncertainties in the internal- and external resistances.

Calculating X_C (to 3 s.f.) and ΔX_C produces Table 5. And plotting those points produces Figure 5. For showing $X_C \propto 1/f$, Figure 6 displays the relevant curve with a line of best fit. For Figure 6, the first 5, and last 10, elements of Table 5 are omitted, this is justifiable from the limitations of the oscilloscope, where peak-to-peak V_C cannot exceed 3.50 V – resulting in an upper limit for V_C , the effects of which can be observed in Figure 3. Noise at higher frequencies is the cause of the omission of the last 10 elements, where the oscilloscope voltage measuring function was taking peak-to-peak vertical noise, not voltage – resulting in a higher-than-accurate value for V_C .

Freq.	X_C	Abs.
mHz	Ω	
200.0	1170	300
400.0	409	100
600.0	239	70
800.0	213	60
1000	167	50
Hz	Ω	
2.000	82.5	20
4.000	42.2	10
6.000	28.9	8
8.000	22.2	7
10.000	18.3	4
Hz	Ω	
20.00	9.33	3
40.00	5.12	1
60.00	3.84	1
80.00	2.85	1
100.0	2.34	1
Hz	Ω	
200.0	1.55	0.4
400.0	1.32	0.4
600.0	0.992	0.3
800.0	0.839	0.3
1000	0.844	0.3
kHz	Ω	
2.000	0.888	0.3
4.000	0.643	0.2
6.000	0.516	0.1
8.000	0.554	0.1
10.00	0.542	0.2
kHz	Ω	
20.00	0.544	0.1
40.00	0.514	0.1
60.00	0.537	0.1
80.00	0.626	0.2
100.0	0.638	0.2
kHz	Ω	
200.0	0.943	0.3
400.0	1.09	0.3
600.0	1.16	0.3
800.0	1.28	0.4
1000	1.70	0.4
MHz	Ω	
2.000	1.88	0.4
4.000	2.44	0.7
6.000	2.77	0.7
8.000	2.82	0.7
10.000	2.80	0.7

Table 5: Capacitive reactance X_C and absolute uncertainties.

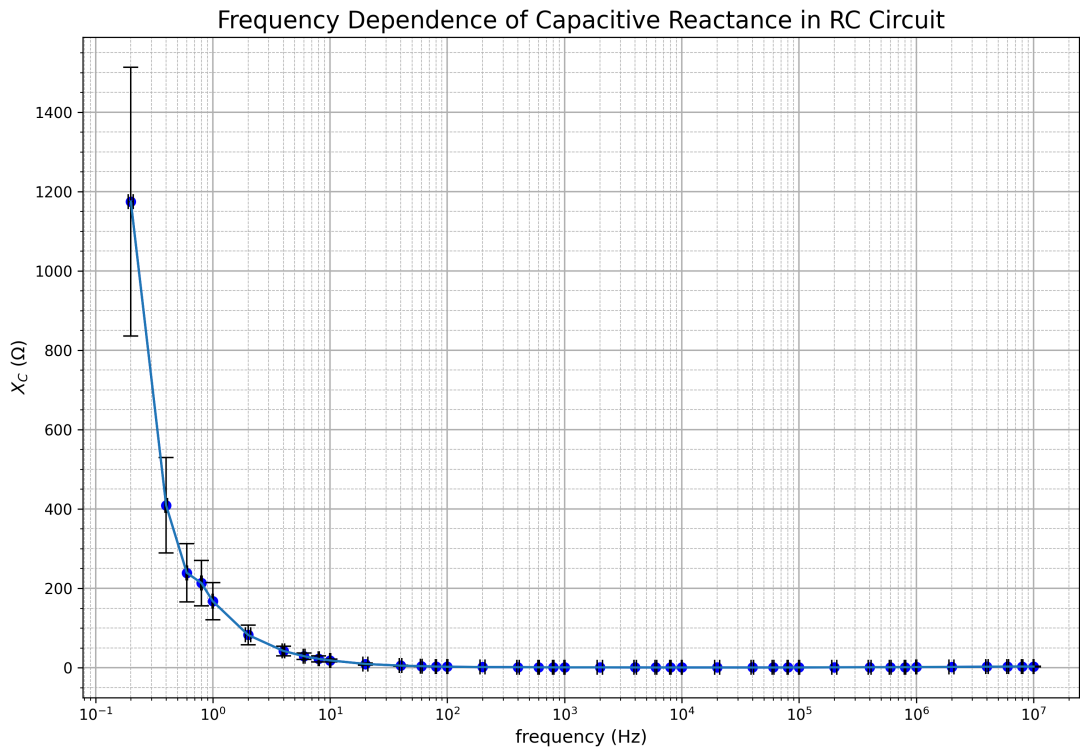


Figure 5: Plotted data from Table 5.

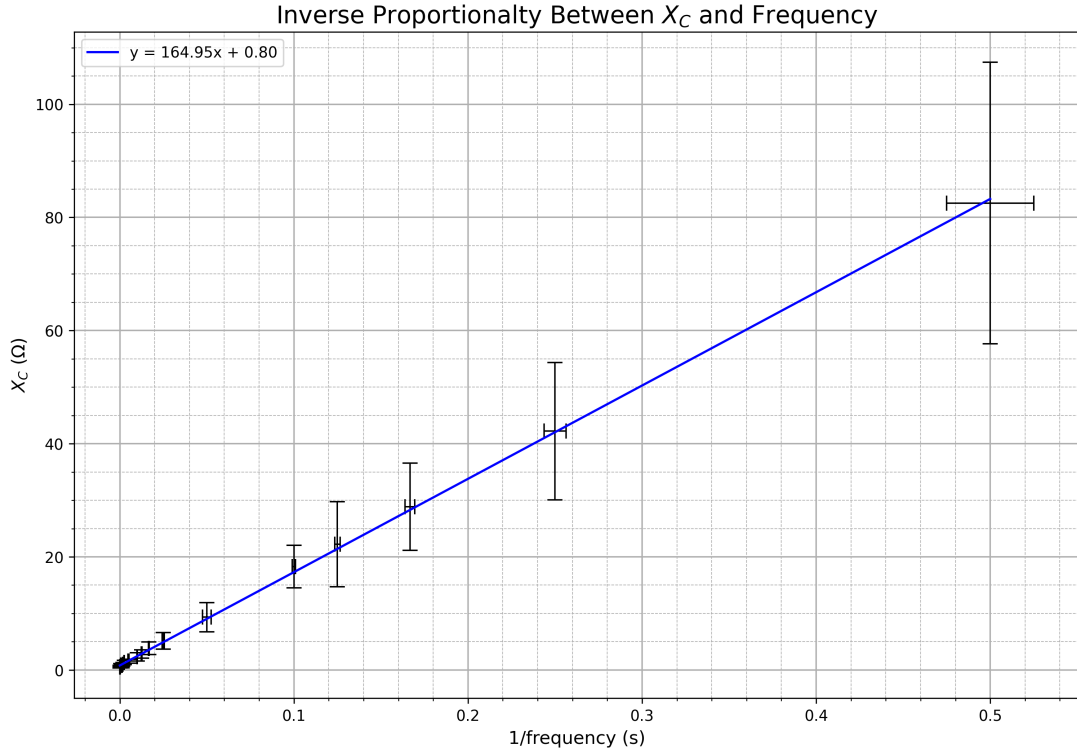


Figure 6: Capacitive reactance plotted against $1/f$.

The equation of the line of best fit in Figure 6 is $X_C = 164.95 \frac{1}{f} + 0.80$. The uncertainty in the gradient is 0.8, and the uncertainty in the y-intercept is 0.09.²

To argue a direct proportion, the origin must be included in the y-intercept uncertainty. For Figure 6, the origin is excluded, therefore $X_C \propto 1/f$ cannot be reliably shown. But the closeness can still be appreciated, if anything.

The other part of the story, the gradient, can still be used to show the desired proportionality. Since X_C is said to be $\frac{1}{2\pi f C}$, then the gradient must equal $\frac{1}{2\pi C}$. Using $C = 1000 \mu\text{F} \pm 20\%$, the gradient should be 159 ± 30 . The actual gradient, and its uncertainty, fit firmly within the expected gradient and its tolerance. Therefore, through this, the relationship $X_C = \frac{1}{2\pi f C}$ (plus some unaccounted constant) is proven experimentally.

The next interest in the series RC circuit is the phase relationship between V_C and V_R . Nothing in particular is being proven, but insights can still be gained. The values for

²These uncertainties were calculated with linear regression and error analysis through Python, not with Excel's LINEST function. See [2].

Figure 7, were calculated from the relationship

$$\frac{\phi}{360} = \frac{\Delta t}{T} \quad (8)$$

Where Δt is the time difference between two equivalent points between the V_C and V_R traces, the specific values measured can be found in the time difference column in Tables 1 and 2. Solving for ϕ gives:

$$\phi = 360f\Delta t \quad (9)$$

Equation 9, and its associated combined uncertainty, is used to plot Figure 7.

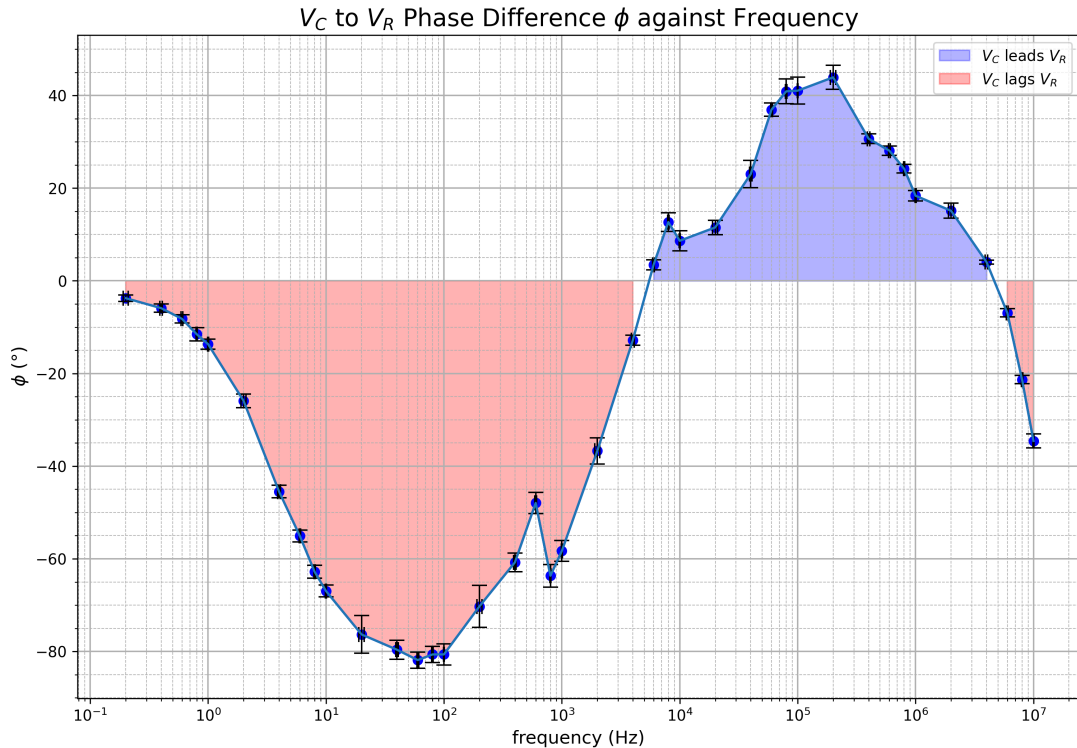


Figure 7: Series RC circuit phase difference between V_C and V_R .

From Figure 7, it is seen that V_C lags behind V_R for lower frequencies, until around 5 kHz, after which the roles reverse, then cross back over after 4 MHz. This is loosely in line with phasor diagrams for RC circuits [6].

1.4.2 Series RL Circuit

The method used for post-processing the series RC circuit can be applied in the same way to series RL circuits, with the necessary adjustments. The V_L and V_R columns from Tables 3 and 4 are plotted below.

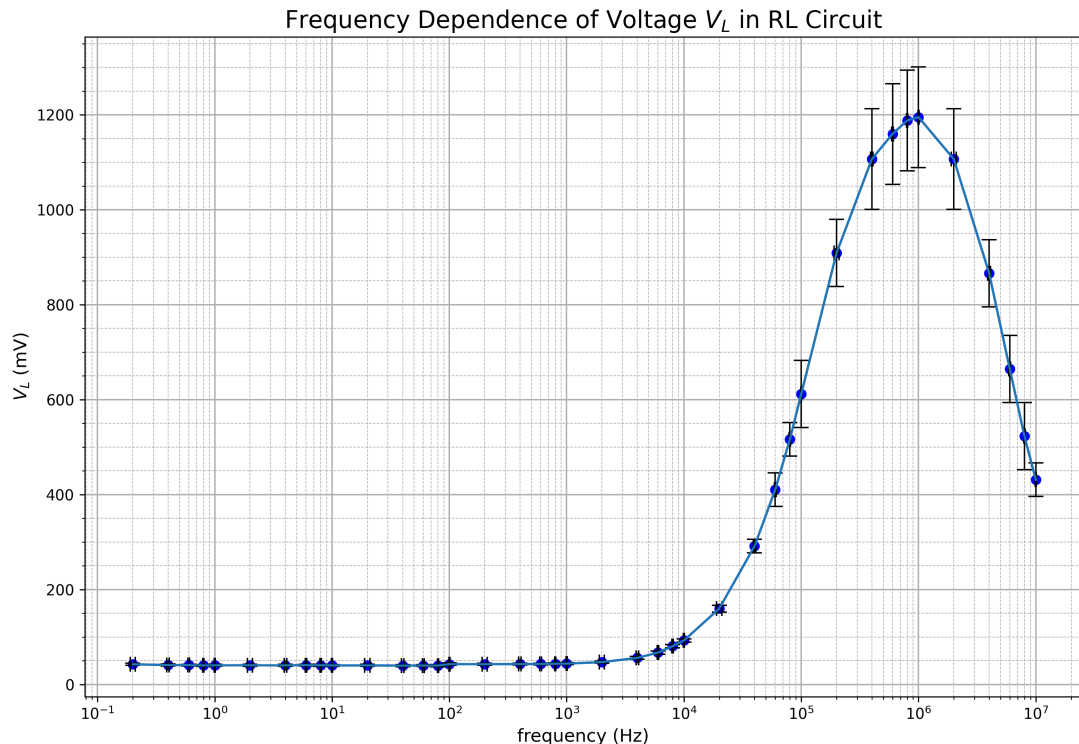


Figure 8: V_L against frequency for series RL circuit.

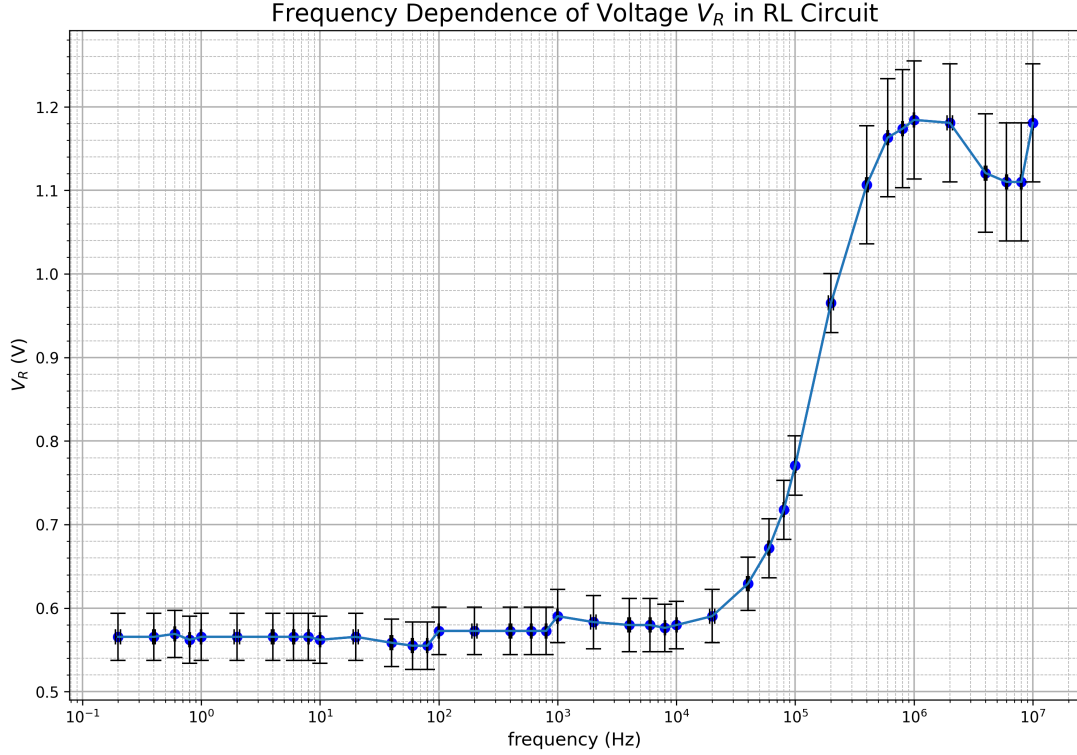


Figure 9: V_R against frequency for series RL circuit.

Observant readers may notice a phallic anomaly in Figure 8 (and partly in Figure 9)... That shouldn't be there. As mentioned earlier, voltage across an inductor should increase with frequency. Keep in mind that this is a semi-log graph, so linear curves don't always appear as straight lines, but the peak is still present in linear graphs. Inductive reactance must be analysed to better understand what is going on in here. But before that, it is worth highlighting the similarities and complementary roles that capacitors and inductors play. Notice how V_L lingers around 50 mV_{rms}, and how V_R lingers around 570 mV_{rms}.

Like before, with the modulus of impedance $|Z|$ in RL circuits being equal to $\sqrt{R^2 + X_L^2}$, X_L can be shown to be:

$$X_L = \frac{V_L R}{\sqrt{V_t^2 - V_L^2}} \quad (10)$$

With associated absolute combined uncertainty:

$$\Delta X_L = X_L \sqrt{2 \left(\frac{\Delta V_L}{V_L} \right)^2 + \left(\frac{\Delta R}{R} \right)^2} \quad (11)$$

Table 6 is the result of these calculations.

Freq.	X_L	Abs.
mHz	Ω	
200.0	3.05	0.3
400.0	2.94	0.3
600.0	2.94	0.3
800.0	2.88	0.3
1000	2.90	0.3
Hz	Ω	
2.000	2.91	0.3
4.000	2.89	0.3
6.000	2.93	0.3
8.000	2.92	0.3
10.000	2.88	0.3
Hz	Ω	
20.00	2.89	0.3
40.00	2.85	0.3
60.00	2.87	0.3
80.00	2.86	0.3
100.0	3.08	0.3
Hz	Ω	
200.0	3.06	0.3
400.0	3.09	0.3
600.0	3.10	0.3
800.0	3.14	0.3
1000	3.16	0.3
kHz	Ω	
2.000	3.39	0.3
4.000	4.03	0.4
6.000	4.84	0.4
8.000	5.81	0.5
10.00	6.68	0.5
kHz	Ω	
20.00	11.6	0.9
40.00	21.6	2
60.00	31.3	4
80.00	40.8	4
100.0	50.6	9
kHz	Ω	
200.0	96.3	10
400.0	178	30
600.0	239	30
800.0	305	40
1000	331	40
MHz	Ω	
2.000	178	30
4.000	87.2	10
6.000	56.7	9
8.000	41.5	8
10.000	33.1	4

Table 6: Inductive reactance X_L and absolute uncertainties.

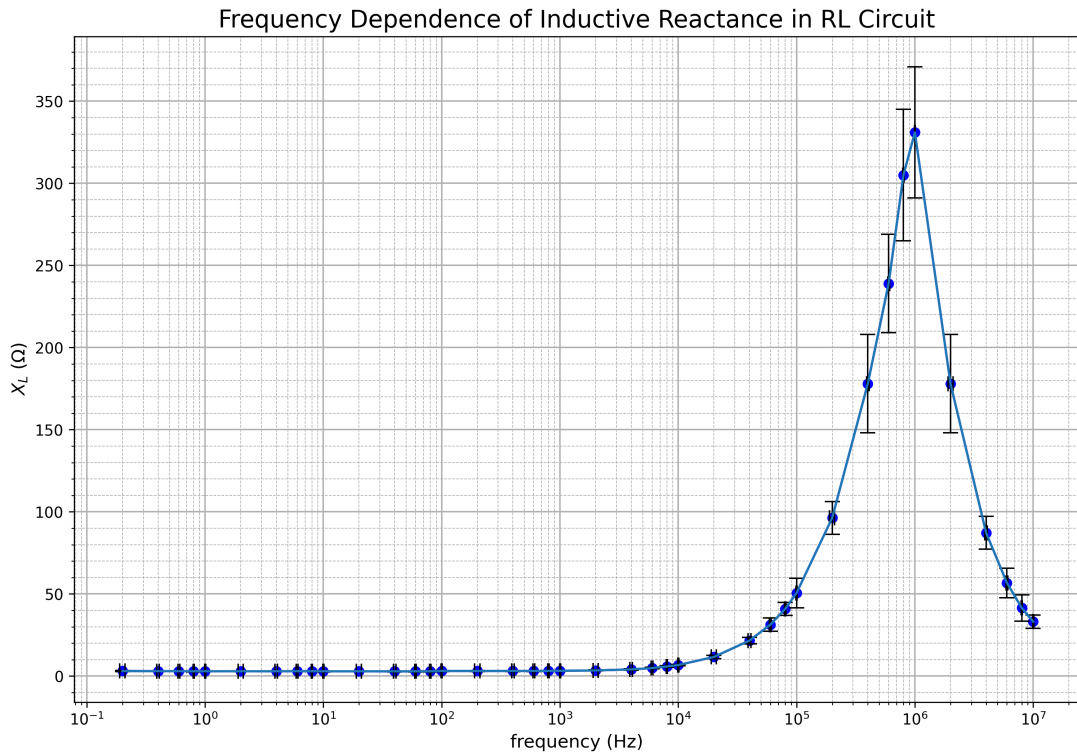


Figure 10: Plotted data from Table 6.

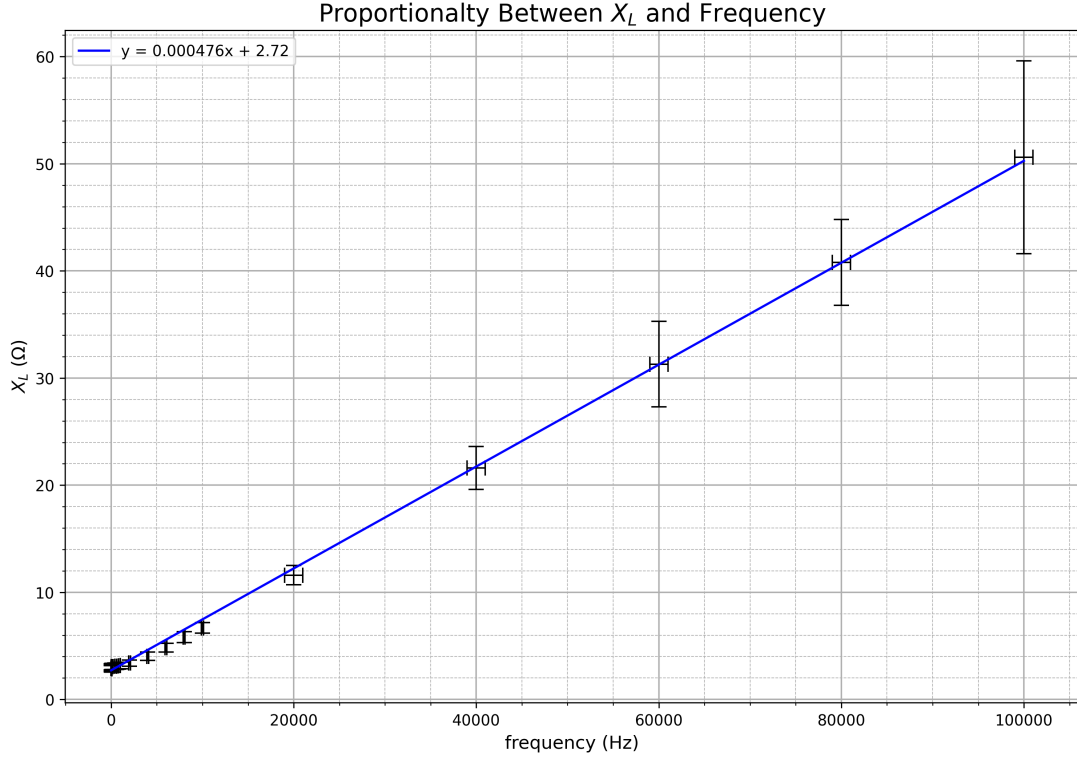


Figure 11: Inductive reactance plotted against f .

Figure 10 still bears the sharp spike, now spikier than ever. From this, it is clear that the circuit is in resonance at 1 MHz. This effect appears one experiment too early and is indicative of a hidden capacitance somewhere within the circuit. This concept will be explained in greater detail in Section 2. For now, using $f_0 = \frac{1}{2\pi\sqrt{LC}}$, C can be solved for with $L = 100 \mu\text{H} \pm 5\%$. Doing so gives $C = 253 \text{ pF} \pm 10 \text{ pF}$. The source of this *parasitic* capacitance [7, p. 255] may be from within the digital oscilloscope. [8] shows schematics of the oscilloscope in use, where multiple capacitors can be seen. However, it is more likely that the capacitance comes from the circuit itself, perhaps between the teeth of the crocodile clips or screws in the terminal blocks.³

Moving onto Figure 11, getting a straight line demanded a '*penectomy*' of the last 10 elements. Even so, the y-intercept of 2.72 ± 0.07 is a major obstacle in proving $V_L \propto f$.

Like for the RC circuit, the gradient might help show $X_L = 2\pi f L$. The expected gradient is $2\pi f$, which equals to 0.000628 ± 0.000003 . The actual gradient is 0.000476 ± 0.000003 . There is no overlap in these values. Therefore, $X_L = 2\pi f L$ cannot be firmly shown experimentally from the data gathered here.

³IDK TBH.

Swiftly ignoring this, the phase difference between V_L and V_R will be explored. The same method from the RC circuit is used here to plot Figure 12.

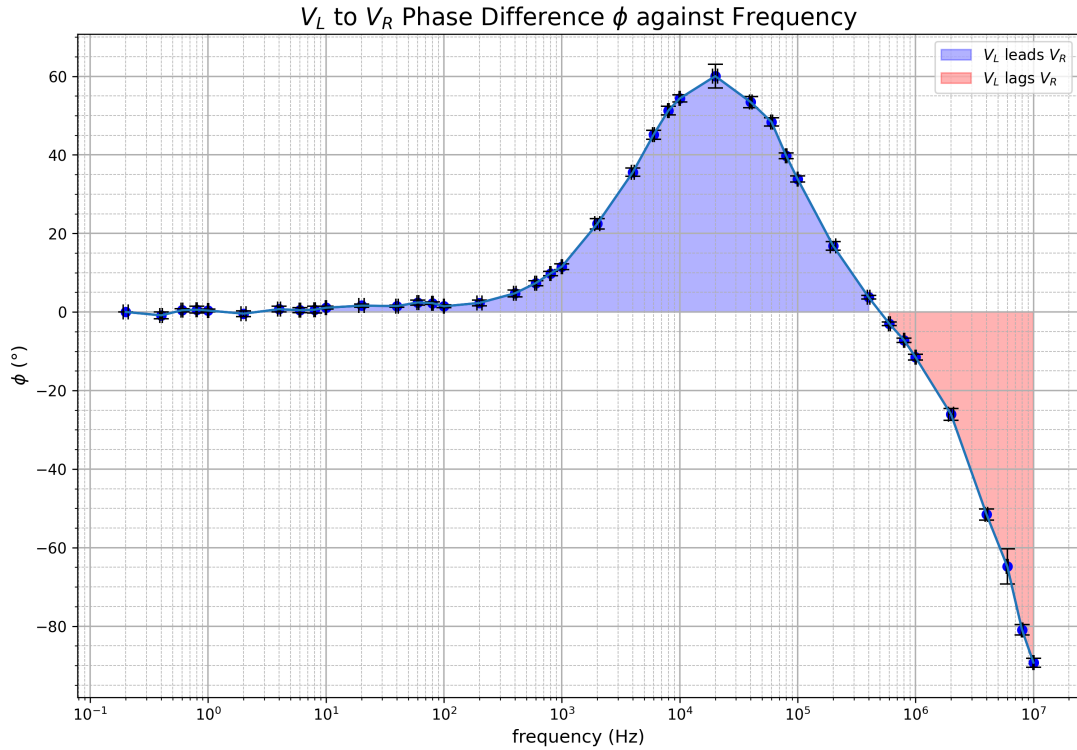


Figure 12: Series RL circuit phase difference between V_L and V_R .

For the lower frequency range, V_L and V_R remain fairly in-phase. This makes intuitive sense, as X_L and V_L are smaller at lower frequencies. This means that the vector sum of V_L and V_R remains very close to V_R , and since the inductor's behaviour approaches that of a resistor at small frequencies, no phase difference is observed. At higher frequencies, the phase difference follows less identifiable structure, probably due to the resonance which inflates both V_L and V_R .

1.4.3 Resonance Inquiry

The final use of the data gathered here is to answer the question: is resonance a strictly dual-component phenomenon, or can it be predicted from separate RC and RL circuits? In RLC circuits, resonance occurs when $X_C = X_L$ (further discussion found in Section ??). So, if resonance can be derived from separate RC and RL circuits, then the resonance frequency must occur where X_C and X_L intercept. This is equivalent to where the difference between the two is zero, as shown in Figure 13.⁴

⁴The first 5 and last 10 elements of each data set is omitted to produce a clearer graph.

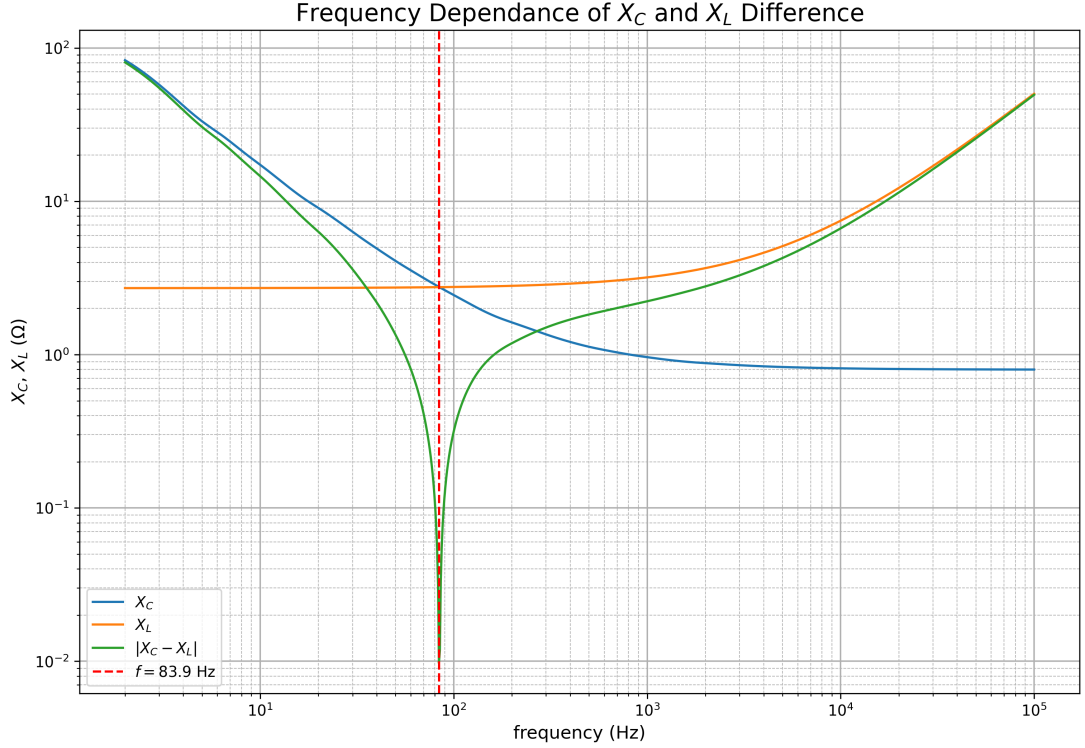


Figure 13: X_C and X_L plotted together.

Following through with the previous logic, the resonance frequency f_0 should be around 83.9 Hz. Using $f_0 = \frac{1}{2\pi\sqrt{LC}}$, the actual resonance frequency of the components should be $503 \text{ Hz} \pm 50 \text{ Hz}$. This is nowhere near 83.9 Hz, so it is safe to say that resonance *is* strictly a dual-component effect.

Note: the uncertainty in the resonance frequency Δf_0 is:

$$\Delta f_0 = \frac{f_0}{2} \sqrt{\% \Delta L^2 + \% \Delta C^2} \quad (12)$$

2 Series and Parallel RLC Circuits

Aims: Verify $f_0 = \frac{1}{2\pi\sqrt{LC}}$ and the nature of resonance peaks in series and semi-parallel resonance circuits. Analyse and understand the phase relationship between difference components in both systems.

2.1 Underlying Physics

Resonance, defined as “a phenomenon in which an oscillator responds most strongly to a driving force that matches its own natural frequency of vibration” [9]. In most cases, when discussing resonance, mechanical resonance is what is being referred to (such as with pendulums or tuning forks). Electrical resonance (RLC) circuits are often overlooked, despite their application in so many areas: radio tuning, AC-to-DC conversion, MRI machines, induction heaters, transmon qubits, tesla coils, etc.

There are two versions of the resonance circuit – series and parallel. The series version works with an inductor and capacitor (and resistor) connected in series, when the capacitor discharges through the inductor, an AC of constant frequency is produced, known as the circuit’s natural frequency [10]. This is possible since the capacitor discharges current in the opposite direction that it charges and since the inductor follows Lenz’s law to oppose changes in current. The result is energy being tossed between capacitor and inductor.

Mathematically, resonance is dictated by the total impedance of a series RLC circuit [11, p. 1-56]:

$$Z = R + j(X_L - X_C) \quad (13)$$

Where j is the imaginary number. The modulus and argument of Z are as follows:

$$|Z| = \sqrt{R^2 + (X_L - X_C)^2} \quad (14)$$

$$\theta = \tan^{-1} \left(\frac{X_L - X_C}{R} \right) \quad (15)$$

Note: θ is the phase difference between circuit current and circuit voltage [12], so cannot be used to analyse the following phase difference graphs between different voltages. From Equations 13 and 14 minimum circuit impedance must occur when $X_L = X_C$. Equating $X_C = \frac{1}{2\pi f C}$ and $X_L = 2\pi f L$ give the expected resonance frequency f_0 of the circuit:

$$f_0 = \frac{1}{2\pi\sqrt{LC}} \quad (16)$$

For the parallel variant of the form in Figure 14, impedance across the LC branches is given by:

$$Z_{LC} = \left(\frac{1}{Z_L} + \frac{1}{Z_C} \right)^{-1} \quad (17)$$

Substituting $Z_L = j\omega L$ and $Z_C = \frac{1}{j\omega C}$, where $\omega = 2\pi f$, and simplifying gives:

$$Z_{LC} = \frac{j\omega L}{1 - \omega^2 LC} \quad (18)$$

At resonance, $\omega_0 = \frac{1}{\sqrt{LC}}$, this value blows up to infinity, meaning no current should be able to flow through the LC branches at resonance, so voltage must also be at a minimum value. It should behave as an open circuit.

Note: the circuit used is not exactly a *parallel* RLC circuit, as there is no separate resistor branch, but its properties are still worth investigating.

2.2 Experiment Description

For this experiment, different values for L and C are used. This is to ensure an adequate quality Q factor for the circuit. Where $Q = \frac{1}{R} \sqrt{L/C}$ for a series RLC circuit. For a parallel RLC circuit, it is the reciprocal. The higher this value, the more distinct the resonance peaks will be. Using the previous L and C values would result in a (series) Q of 0.00355. But using $L = 1 \text{ mH} \pm 5\%$ and $C = 470 \text{ pF} \pm 10\%$ gives a much higher Q of 16.4.

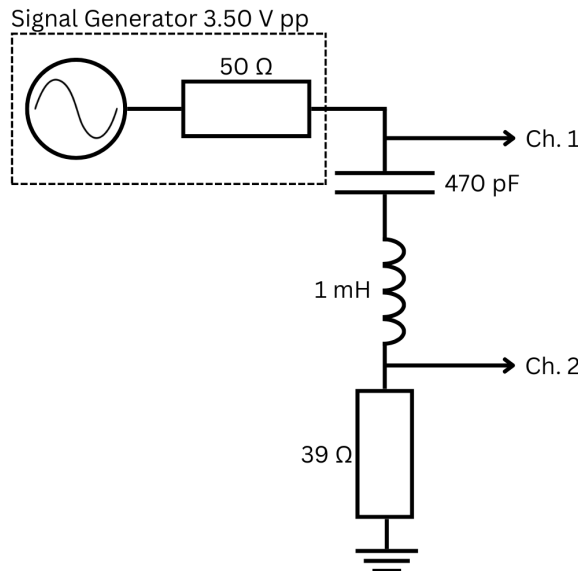
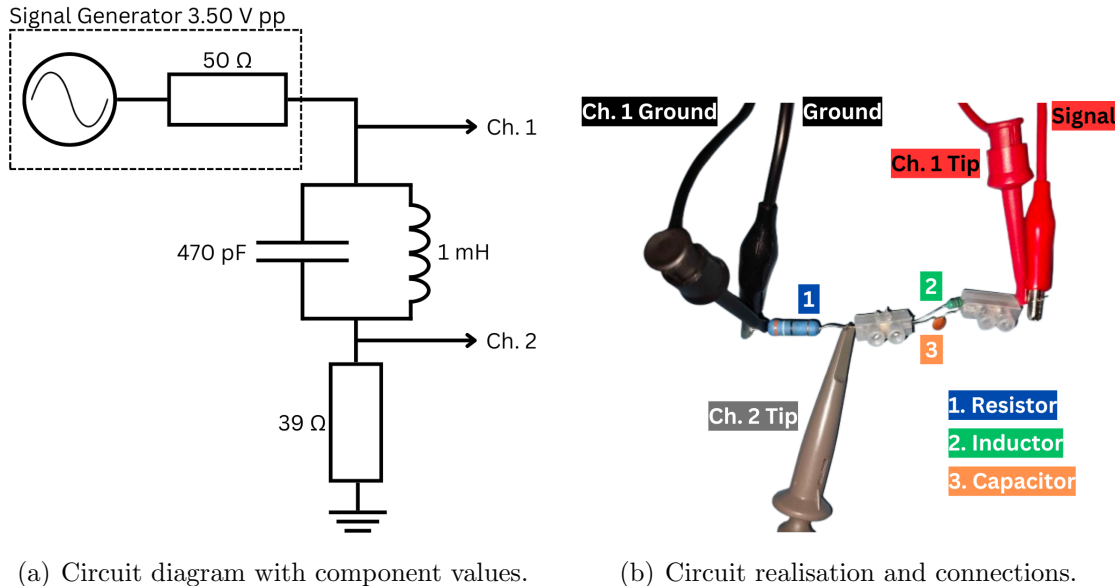


Figure 14: Series RLC circuit diagram.

With these new components, the same process of experimentation has been followed. Figures 14 and 15 show how the components were connected, and Tables 7 through 9 show what values were extracted. The difference this time is less data points have been collected. Through rough calculation, resonance should only occur at higher frequencies, so measurements start from 20 kHz. The values around the expected resonance frequency, $232 \text{ kHz} \pm 10 \text{ kHz}$, were also honed in on, to ensure a peak is derived from the data. However, the following graphs show that this was pointless.



(a) Circuit diagram with component values.

(b) Circuit realisation and connections.

Figure 15: Parallel RLC circuit diagrams.

For the series RLC case, an additional measurement, the phase difference between V_C and V_L , was made. This was done by moving the channel 1 oscilloscope tip between the capacitor and inductor.

For further clarification, the branches in the parallel RLC circuit were made by placing the inductor and capacitor across the same two terminal blocks. More sophisticated methods exist.

2.4 Discussions and Conclusions

2.4.1 Series RLC Circuit

Given that resonance was observed in the RL circuit, it is not surprising that coupled resonance [3, pp. 157–158] is present for the following circuits.

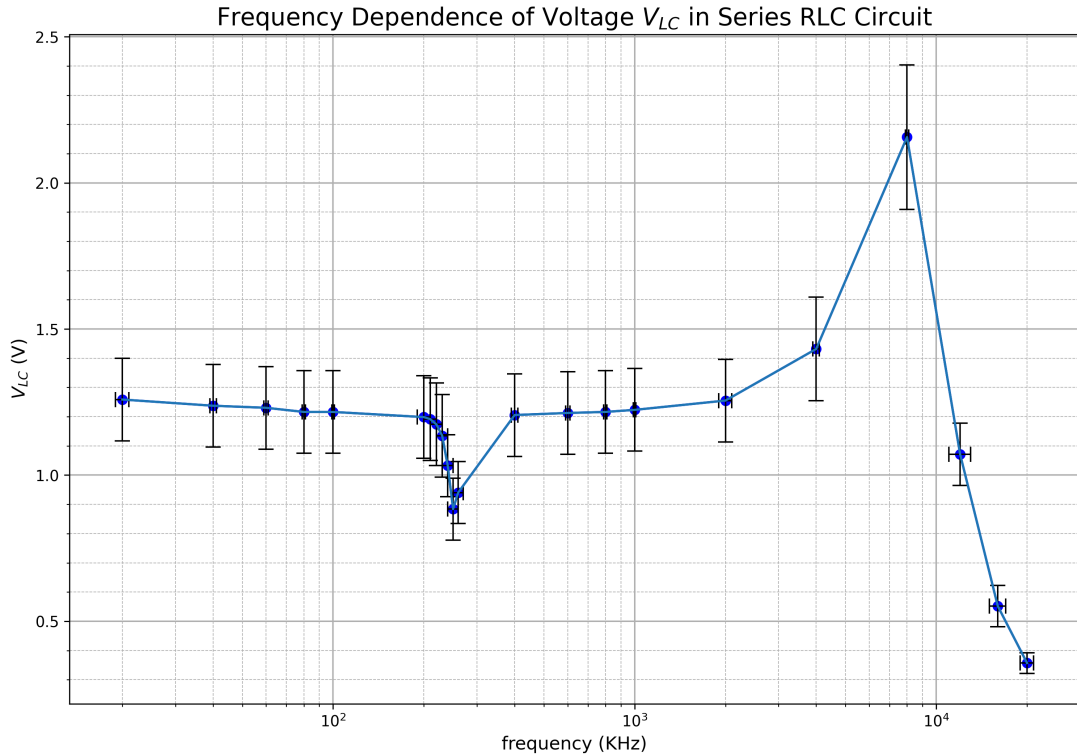


Figure 16: V_{LC} against frequency for series RLC circuit.

This graph clearly shows resonance splitting. With anti-resonance (minimum) at around 250 kHz with an rms voltage of just under 0.9 V and resonance (maximum) with 8 MHz at around 2.2 V. What is particularly interesting about these results, aside from the funky shape, is that the peak-to-peak voltage measured (reaching 6.10 V_{pp} in Table 7) exceeded the output voltage of 3.50 V_{pp}. This is called *voltage amplification* and is a product of the high Q factor – resulting in a sharp, narrow, and tall resonance peak.

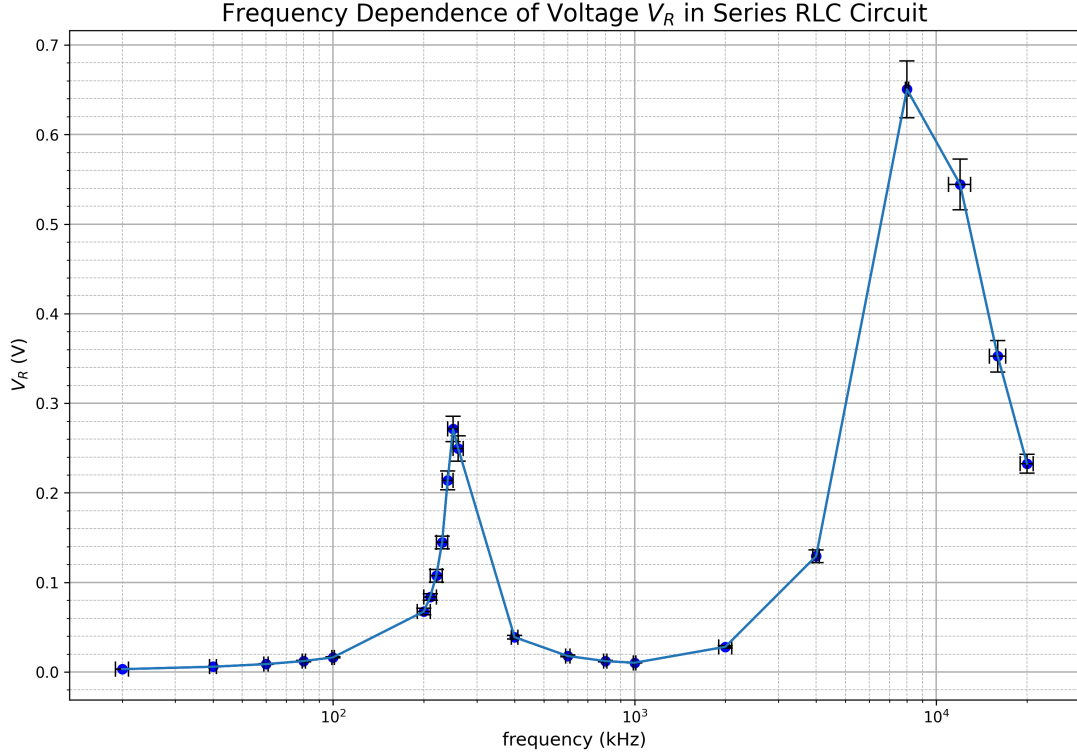


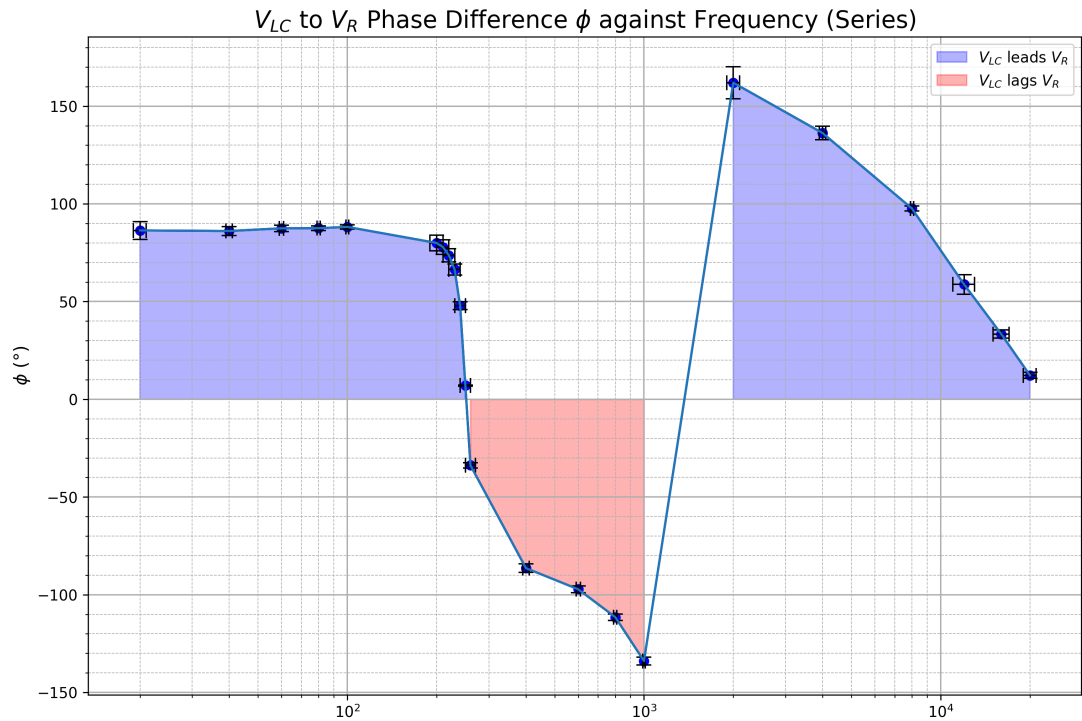
Figure 17: V_R against frequency for series RLC circuit.

Figure 17, showing V_R against frequency, is a much cleaner example of resonance splitting, as both are maximums. The points of resonance are the same for V_{LC} .

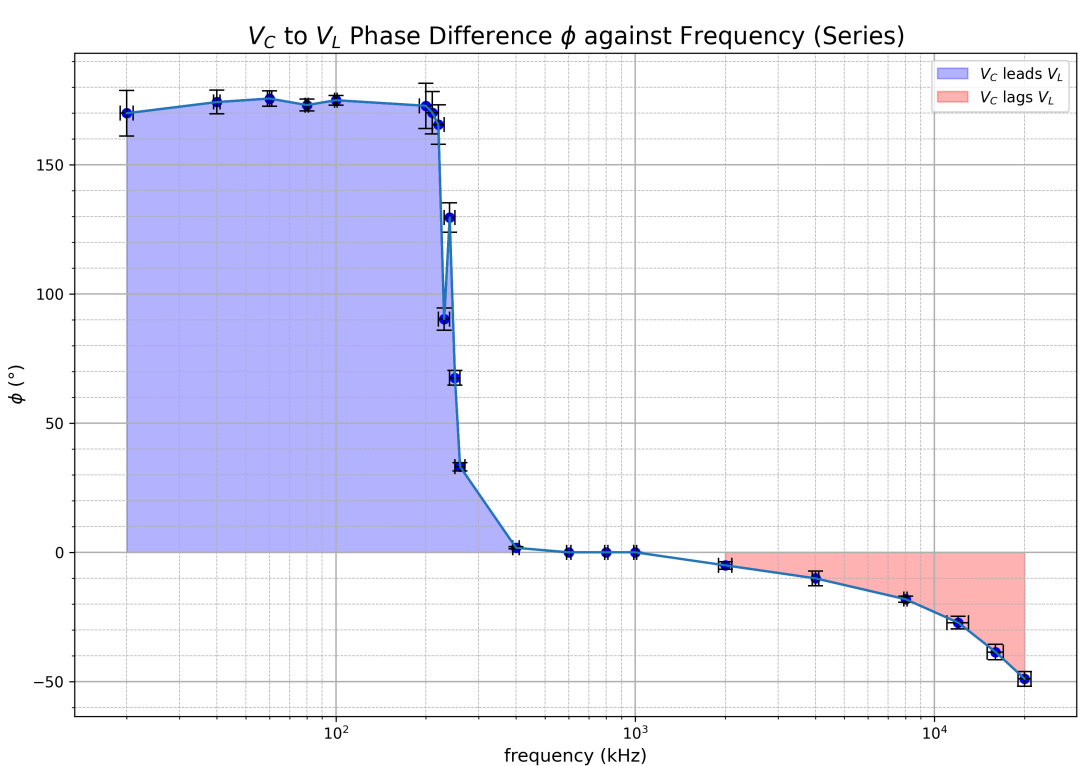
Coupled resonance circuits occur when additional L or C components are introduced to the original RLC combination. In this case, it is likely an extra capacitive component, as seen by the parasitic capacitance in the RL circuit. Though a greater total capacitance should result in a lower f_0 , whereas in Figures 16 and 17, both resonances occur at a greater-than-expected value. Another possible explanation is the resonances observed are the harmonics of the actual resonance. This theory is backed by the fact the second resonance peak occurs at a frequency which is an integer multiple (32) of the first (fundamental) frequency – but this is likely just a result of the experimental intervals used. Another argument for this theory is that capacitors exhibit nonlinearity⁵ when high voltages are applied to them, which is the case at resonance due to the observed voltage amplification.

As always, the phase relationships between components is explored. Through the same methods as before, the following graphs were created:

⁵Components are non-linear when they don't show a linear relationship between current and voltage [13, pp. 1–2]. This is needed for harmonics to form.



(a) V_{LC} to V_R .



(b) V_C to V_L .

Figure 18: Series RLC circuit phase differences.

In both graphs⁶, the phase difference undergoes a change between the resonance values for the circuit. Figure 18(a) shows V_{LC} consistently leading V_R by around 90° , before suddenly starting to lag after the first resonance peak. As frequency increases further, V_{LC} begins to lead again, just before the second resonance, but its lead is not kept constant. It is worth noting that the jump from -135° to around 160° may actually be a jump from -135° to -200° .

Figure 18(b) shows another interesting pattern, with V_C and V_L being almost completely out of phase at low frequencies, to then being perfectly in phase at frequencies between the two resonance frequencies. beyond which, V_L slowly begins to lead V_C as frequency is increased.

2.4.2 Parallel RLC Circuit

For the semi-parallel RLC circuit, Figures 19 and 20 were produced (from Table 9).

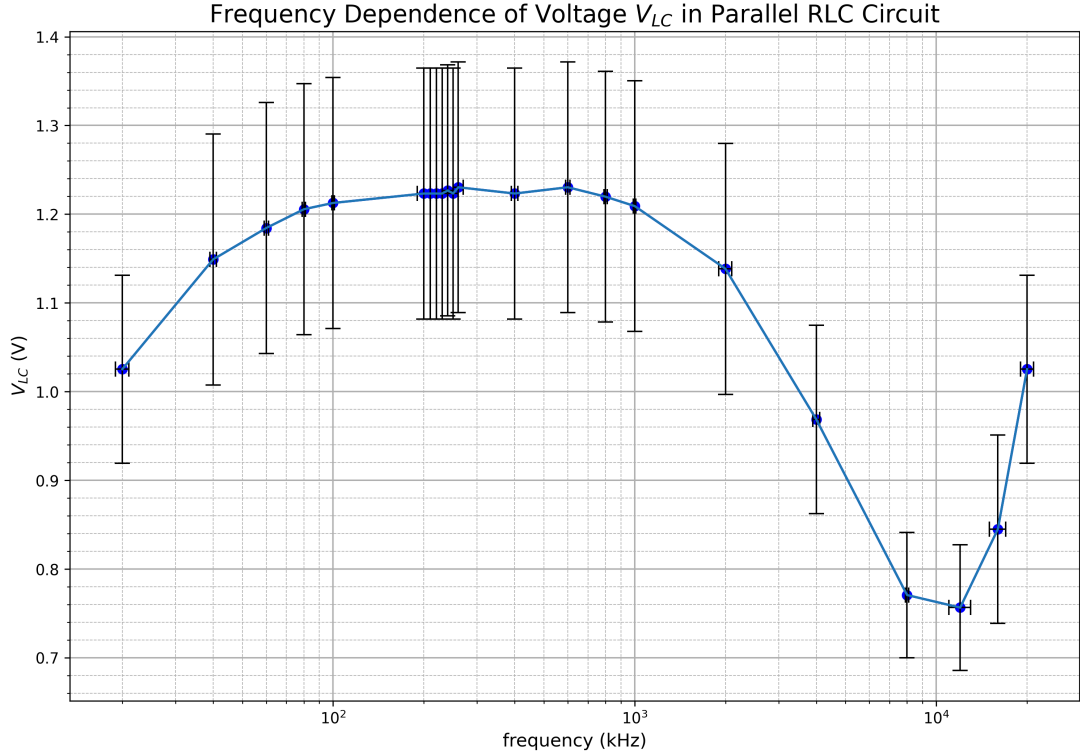


Figure 19: V_{LC} against frequency for parallel RLC circuit.

Like with all comparisons to parallel and series circuits, Figure 19 is the complement of Figure 16. At 250 kHz there is resonance (maximum) and at around 8 MHz there is anti-

⁶The unfilled regions are a limitation of Matplotlib.

resonance (minimum). It should be clear that the actual resonance value will be between 8 and 12 MHz. Another point of comparison is that the resonance peaks themselves are much wider. This is due to the Q factor in parallel RLC circuits being the reciprocal of series: $Q_{parallel} = R\sqrt{C/L}$. This produces a Q of 0.061.

Figure 20 breaks this complementary pattern, instead of two minimum, it displays a minimum followed by a maximum. The minimum shown is very substantial, with rms voltage dropping *very* close to 0 – this verifies that circuit impedance grows massively at resonance in parallel circuits.

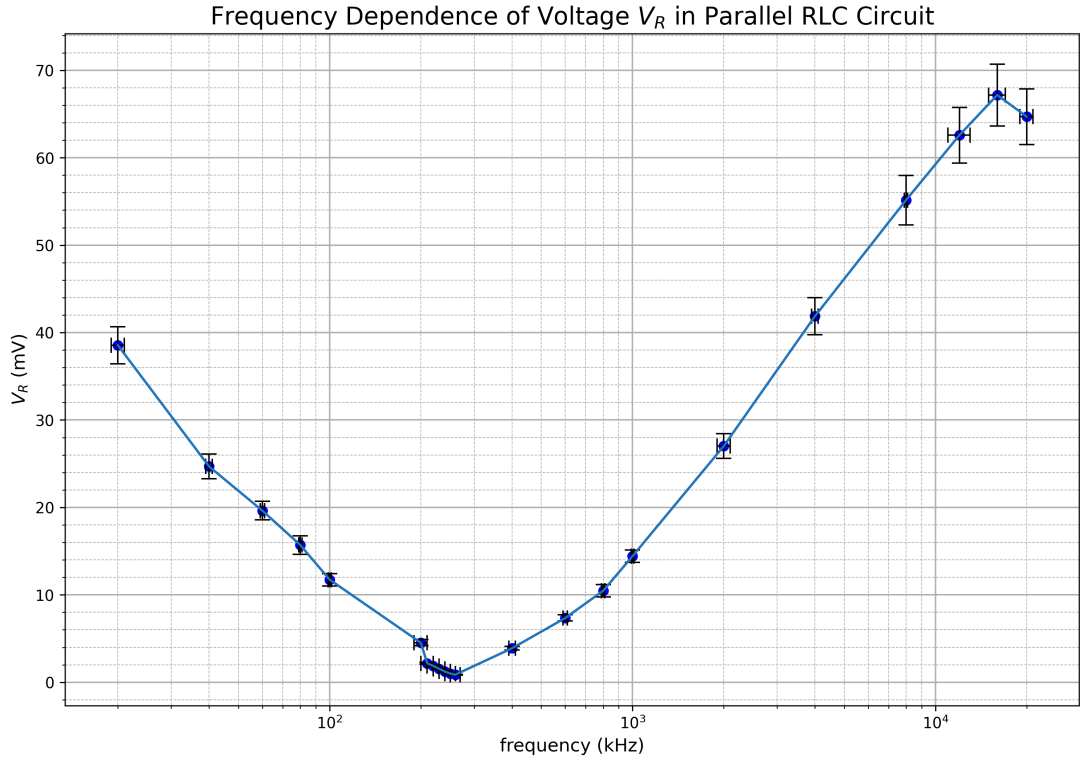


Figure 20: V_R against frequency for parallel RLC circuit.

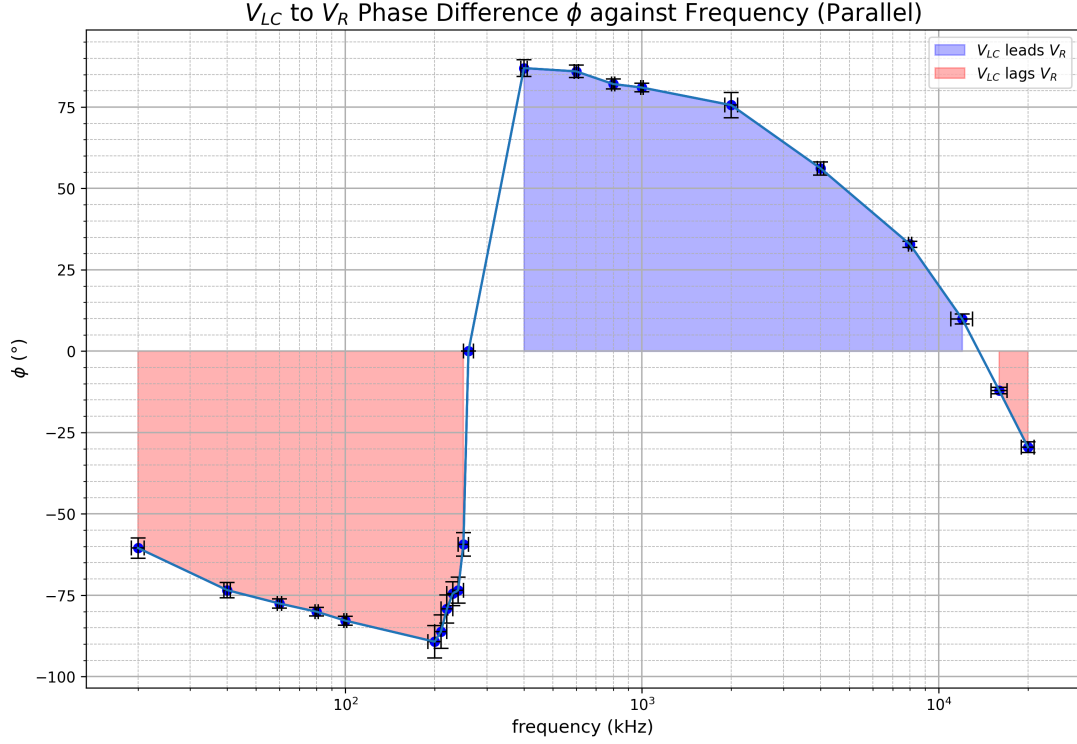


Figure 21: Data from Table RLCp.

For the parallel RLC circuit, only the phase relationship between V_{LC} and V_R was tested. This graph loosely reflects that of Figure 18(a), in that phase is reversed with V_{LC} lagging V_R before the first resonance before leading at higher frequencies. At frequencies near and above the second resonance, V_{LC} starts to lag again.

To conclude the second experiment, the relationship $f_0 = \frac{1}{2\pi\sqrt{LC}}$ could not be verified from the data gathered. However, the nature of some of the resonance peaks were verified (such as voltage in parallel RLC circuits dropping to near zero at resonance (half of the time)). Finally, the phase relationships between different components were explored, though no deep analysis was given.

3 Series RLC Transient Responses

Aims: Understand the behaviour of a series RLC circuit after being sent a single AC pulse. Find the damped natural frequency of the circuit and compare the value with the theorised resonance frequency. Verify that the type of damping produced depends on the resistance of the circuit.

3.1 Underlying Physics

If a force is applied to an oscillatory system, such as a pendulum, the system will oscillate at its natural frequency. This frequency is a different concept from the resonance frequency:

- Resonance frequency: frequency of a driving force that causes maximum amplitude of oscillations in the system.
- Natural frequency: the frequency at which a system oscillates when an initial force is applied, then removed.

When an initial force is applied, then removed, to an oscillatory system, the amplitude of its oscillation will decrease with time, this is known as damping. For the pendulum example, the source of the damping is the air resistance opposing its motion. There are three types of damping: underdamped, critically damped, and overdamped. The damping experienced for a particular system is dependant on the nature of the solution to the differential equation describing its motion [14, pp. 4–5].

Returning to the series RLC system, its differential equation (with charge being the dependant variable) can be derived using Kirchhoff's voltage law (the sum of voltages across components in a series circuit equals the supply voltage):

$$V_L(t) + V_R(t) + V_C(t) = V(t) \quad (19)$$

Substituting in $V_L(t) = L \frac{dI(t)}{dt}$, $V_R(t) = I(t)R$, $V_C(t) = \frac{Q(t)}{C}$, and $V(t) = 0$ (since this is for an undriven system), gives:

$$L \frac{d^2Q(t)}{dt^2} + R \frac{dQ(t)}{dt} + \frac{1}{C} Q(t) = 0 \quad (20)$$

This is a homogenous second-order ODE, with its solution dependant on the discriminant, $\Delta = R^2 - 4L/C$, of its auxiliary equation $Lm^2 + Rm + \frac{1}{C} = 0$.

When $\Delta < 0 \Leftrightarrow R < 2\sqrt{L/C}$, the solution will be of the form $y = e^{px}(A \sin qx + B \cos qx)$, with roots $p \pm qj$, where p must be negative. This graphs to an exponentially decreasing waveform – underdamped motion.

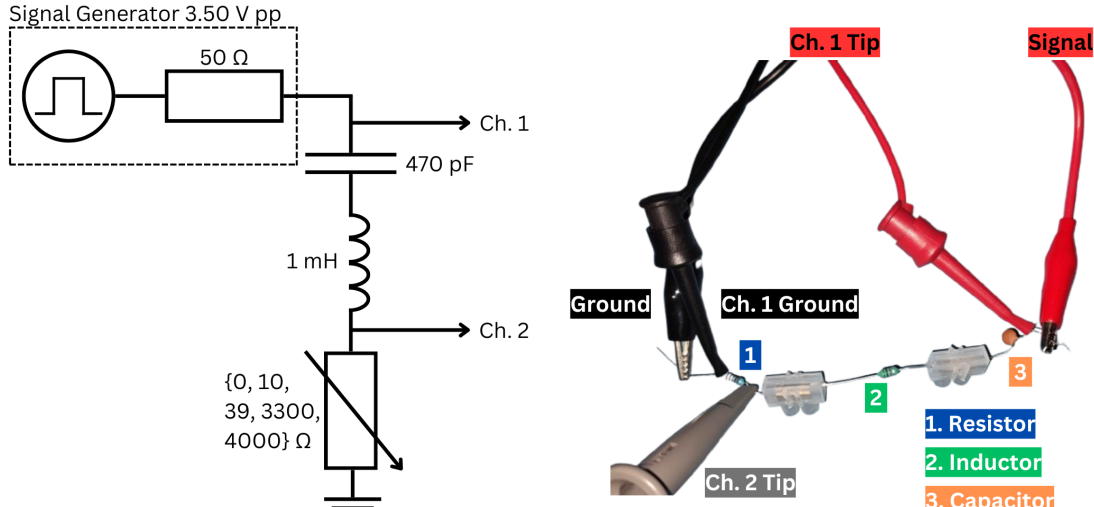
The second scenario, $\Delta = 0 \Leftrightarrow R = 2\sqrt{L/C}$, has a solution of the form $y = e^{mx}(A + Bx)$, where m is a repeated root. This corresponds to a critically-damped system, with a decay curve reaching 0 in minimum time.

The final option, for an overdamped system with no oscillations, and a curve that *gradually* drops to 0, happens when $\Delta > 0 \Leftrightarrow R > 2\sqrt{L/C}$. The solution to this will be in the form $y = Ae^{m_1 x} + Be^{m_2 x}$, where m_1 and m_2 are the distinct roots.

3.2 Experiment Description

The procedure for this experiment is best suited for a variable resistor, where resistance values can be finely selected. However, in this case, individual resistors were used (from a lack of precisely-controllable variable resistors on hand). To decide on which values of resistance to use, the critical resistance R_c must be calculated, this occurs with $R_c = 2\sqrt{L/C}$. For the same L and C values used in the previous experiment, R_c should be 2920Ω , therefore the external resistance value will be 2870Ω .

Resistances lower than that were used for the underdamped circuits: one with no resistor, one with a $10 \Omega \pm 5\%$ resistor, and another with the $39 \Omega \pm 5\%$ seen previously. For the critically-damped circuit, the closest resistance value easily found was $3.3 \text{ k}\Omega \pm 1\%$. Two $2 \text{ k}\Omega \pm 1\%$ resistors connected in series were used for the overdamped circuit.

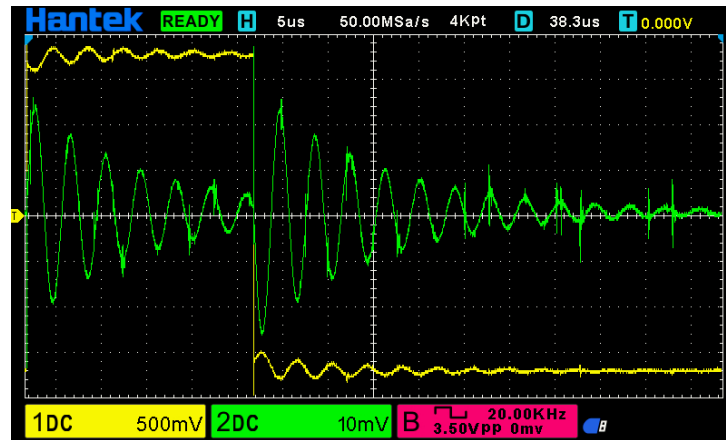


(a) Circuit diagram with component values. (b) Circuit realisation and connections.

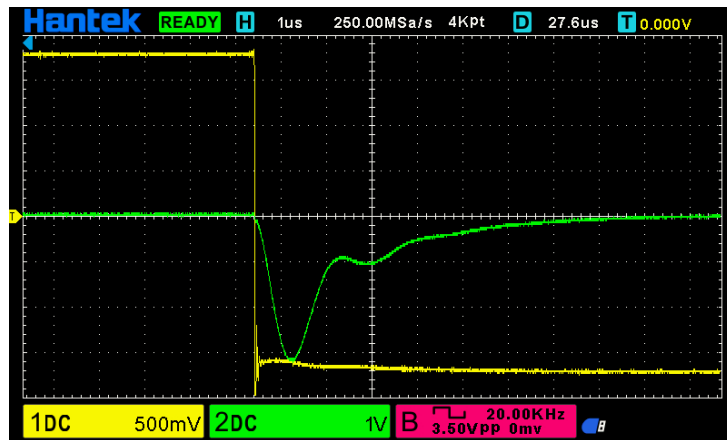
Figure 22: Series RLC transient response circuit diagrams.

The signal generator, as indicated by Figure 22, was set to produce a single square wave output. The frequency of this pulse was set to 20 kHz to allow ample time for components to fully charge.

After the pulse wave was sent, the oscilloscope screen was set to capture the voltage traces – only values from channel 2 were recorded. For the underdamped circuits, the voltage peaks were measured with the cursor (from 0 to extremum), each subsequent peak was measured until they faded into noise close to zero (either 10 or 18 extrema were measured per resistor value). The period of each oscillation was measured, the tables for this are not recorded here, by the final measurement and absolute uncertainty is $3.87 \mu\text{s} \pm 0.05 \mu\text{s}$. The settling time for the response was also measured, from the moment the pulse passed, to voltage dropping to zero(ish). For the critically- and overdamped circuits, the initial peak voltages were measured (0 to extremum) and the circuits' settling times.



(a) Underdamped response.



(b) Overdamped response.

Figure 23: Oscilloscope screenshots of transient responses (green trace).

3.4 Discussions and Conclusions

3.4.1 Underdamped Circuits

As mentioned, the period of oscillations was found to be $3.87 \mu\text{s} \pm 0.05 \mu\text{s}$, this translated to $258 \text{ kHz} \pm 3 \text{ kHz}$. This is higher than the theorised resonance frequency of $232 \text{ kHz} \pm 10 \text{ kHz}$, but does align pretty close with some of the graphs in Section ?? for the first resonance peak.

From Tables 10 through 12, Figure 24 was plotted. The time spacing between the points wasn't directly measured, but was fitted in accordance with the period calculation and visual cues seen in figure 23(a). Only the y-value uncertainties are included.

What is immediately observed is the shape the points trace out (especially the blue points, $R = 0 \Omega$), which follow an exponential decay, which is in line with general solution to the ODE for all types of damping. The second noticeable thing about the points is that higher resistances reduce the voltage amplitudes for the extrema and the settling times (Table 14) – at least that is the trend for the three resistance values measured.

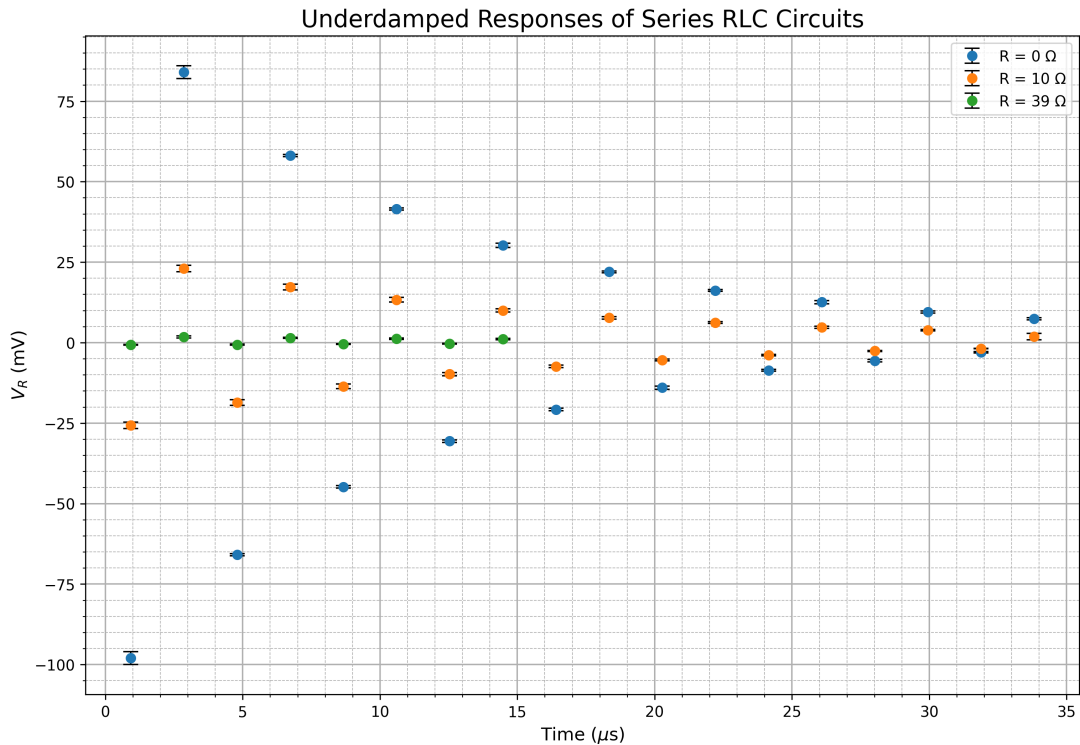


Figure 24: Underdamped Extrema points.

Using SciPy (Python library) modules for interpolation and curve fitting, the equations for the underdamped circuits have been found (to 2 d.p.) and graphed in Figure 25.

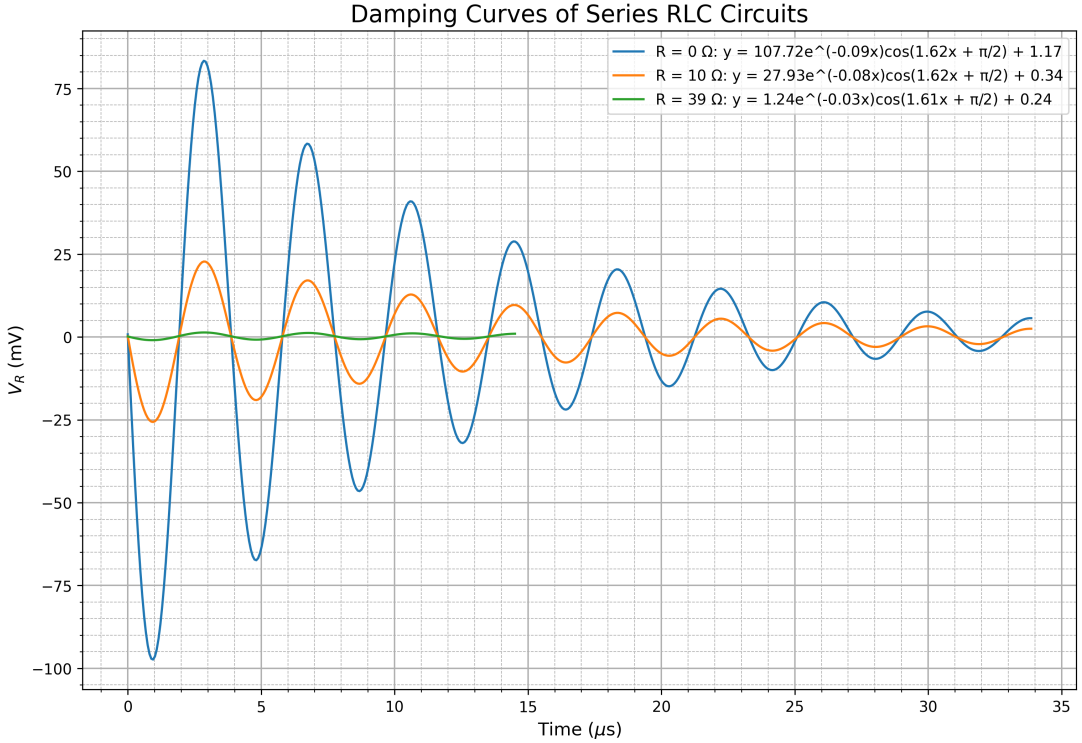


Figure 25: Fitted underdamped curves.

Interpolating and fitting yields the following equations, which have been converted to Volts $V(t)$ and seconds t . $\cos(\omega t + \pi/2)$ has also been converted to $-\sin(\omega t)$.

- $R = 0 \Omega: V(t) = -0.10772e^{-90000t} \sin(1,620,000t) + 0.00117$
- $R = 10 \Omega: V(t) = -0.02793e^{-80000t} \sin(1,620,000t) + 0.00034$
- $R = 39 \Omega: V(t) = -0.00124e^{-30000t} \sin(1,610,000t) + 0.00024$

The solutions are in terms of $V(t)$, not $Q(t)$ as seen in Equation 20. This is fine since these values are proportional.

The most relevant values to analyse in the above equations are the coefficients of t : the damping factor α and the damped natural frequency ω_d . The derivations of these coefficients come from the \Re and \Im components of the auxiliary equation [14, p. 6]:

$$\alpha = \frac{R}{2L} \quad (21)$$

$$\omega_d = \sqrt{\frac{1}{LC} - \frac{R^2}{4L^2}} = \sqrt{\omega_0^2 - \alpha^2} \quad (22)$$

For the first equation, where total resistance is 50Ω , it is seen that $\alpha = 90000$. However, by Equation 21 $\alpha = 25000 \pm 1000$. These values are very far off and, in fact, all calculated

values for the damping factor differ greatly from the approximated value on the fitting curve. This could be from inaccuracies in the code to find the values or due to a lack of data points to properly indicate the nature of the exponential decay.

The next value, the damped natural frequency ω_d , appears constant (since the values for R only slightly deviate), sitting at around 1,620,000. The calculated value for this (using the 50Ω circuit again) is $1,460,000 \pm 100,000$. This calculation is closer relative to the damping factor, but is still different. However, using $\omega = \frac{2\pi}{T}$, ω_d comes out to $1,620,000 \pm 20,000$ which is pretty much perfect. Though this isn't surprising since the curves for Figure 25 were plotted using that specific value for T , $3.87\mu s$. The reason for ω_d being bigger than expected is likely due to parasitic impedance, or some other unaccounted component value, that seems to have messed up all experimental results in this report.

Another thing to note for these results, is all the above equations have a positive constant term. This means that voltage isn't dropping to zero, but a value slightly above zero. This could be explainable by some slight DC offset or floating references [15] from misplaced oscilloscope ground leads.

So, to conclude the underdamped circuits, damped natural frequency has been shown to be different from resonance frequency: theoretically, mathematically and experimentally (for the most part). The form of the underdamped oscillations have also been shown to be of the form of one of the possible solutions to the aforementioned ODE. Where $R < 2\sqrt{L/C}$, voltage exponentially decreases with multiple oscillations, just like with underdamped mechanical systems.

3.4.2 Critically-Damped and Overdamped Circuits

Technically both the other circuits are overdamped systems, since their total resistances are both over the critical resistance of 2920Ω . Though they still have differences that can aid in distinguishing between a critically-damped circuit and an overdamped circuit.

Firstly, from Table 13, the circuit with higher resistance has a larger peak voltage (in terms of magnitude). This breaks the trend seen in the underdamped circuit, and also has a key difference that the peak voltages here are a couple orders of magnitude bigger. With the 3.3 kHz resistor producing a peak voltage of $-2.90\text{ V} \pm 0.04\text{ V}$ and the 2 kHz resistors having a peak voltage of $-3.19\text{ V} \pm 0.05\text{ V}$.

As discussed above, a critically-damped system should return to zero in the minimum amount of time with no oscillations. This fact can be extrapolated with the settling time of the least overdamped circuit being smaller than the most overdamped circuit:

$6.69 \mu\text{s} \pm 0.1 \mu\text{s} < 8.36 \mu\text{s} \pm 0.1 \mu\text{s}$. But this cannot serve as verification, of course.

The final point of discussion for these circuits is that they showed some level of oscillation (see Figure 23(b)), contrary to expectations. This may be due to the evidenced coupled nature of the series RLC circuits used here, as seen from Section 2.

Overall, it is clear that the damping experienced by these circuits are completely different from the underdamped ones. Therefore, it can be justified that resistance does in fact determine the nature of the damping experienced. However, critically- and overdamped systems cannot be properly distinguished.

4 Evaluation of

4.1 Procedures

All measurements taken come from the oscilloscope's measurement functions, so evaluating the accuracy and precision of the procedures really comes down to evaluating the performance of the oscilloscope.

Each experiment, except for the first RC circuit, produced results far off the expected theoretical values, hence they are inaccurate. Potential sources of these deviations are offered in previous sections. The fact the only *accurate* experiment didn't involve any inductor component may hint towards the inductors themselves being the primary source of error and the parasitic capacitance previously mentioned.

The precision of the oscilloscope measurements are more than adequate. The exact precision could be altered using the y-gain and time-base dials, with the limit of precision being the display resolution of the oscilloscope screen. Overall, there are no concerns over precision.

The amount of data gathered (including repeat measurements and ranges) is more than enough (bordering excessive). The repeat measurements ensured a suitably low random uncertainty and a precise final value. The range of data allows for the fullest picture of the behaviour of the circuits to be drawn. Following logarithmic increments also aided in clearer and readable plotting.

The control variables, the circuit components, are adequate also. The values for each were checked against their colour bands. However, the suspicion of the inductors being the source of error was not investigated. To have better control over these variables, the components could have been tested with a multimeter to verify their values are still accurate.

The control over uncertainties could also be improved upon. All components had their associated calibration uncertainty, and the validity of carrying these exact percent uncertainties over to other values is questionable. For example, 5% uncertainty in a capacitor being carried over directly to 5% uncertainty in the voltage across the capacitor.

4.2 Project

The selection of procedures was nothing but sloppy. The importance of LC oscillators in transmon qubits made this topic an easy choice for investigation for me, but deciding on what aspects to investigate was not so easy. The third experiment on transient response was a last-minute decision. The original plan was to build a crystal radio receiver to showcase an application of RLC circuits, but this was soon abandoned.⁷ In the end, the easy route of investigating transience was picked.

The only real problem overcome in this project was in sourcing a signal generator and an oscilloscope that met the demands of the investigations. The ones from school were ****, but I was fortunate enough to have a sparky of a brother who lent me one of his digital oscilloscopes, which simultaneously solved both problems.

The main downside to this project is the lack of variety of measurements made, and the tools used to measure. The oscilloscope was 100% relied upon, either measuring a voltage value or a time value. Current couldn't be measured by the oscilloscope, and all the ammeters on hand failed to give a decent/stable reading on current in the circuits (either from a technical limitation or a human limitation in skill).

Another downside is the poor analysis of results, *especially* for the phase differences in earlier experiments. Clearly! No real explanations were given, just descriptions of the graphs.

The main ways to improve procedures are: to use a better oscilloscope or measurement device; to check components for their values; and to check results frequently to ensure they sound about right.⁸

There are many further avenues of RLC circuits to explore. Such as bandpass filters, actual coupled RLC circuits, LC oscillators (circuits that produce an AC signal), and applications of RLCs. But the clearest way to go is to analyse the phase between voltages of components and current in the circuit.

⁷I came to the realisation that there are two ways building a crystal radio could end. (1) You hear voices across the radio. (2) You hear voices in your head.

⁸I only realised how mystifying my results were during post-processing, by which time it was too late to redeem.

References

- [1] *DSO2000 Series Digital Storage Oscilloscope User Manual*, Hantek, accessed: 12 Feb. 2025. [Online]. Available: <https://hantek.com/products/detail/17182>
- [2] A-n-d-R-o, *Advanced Higher Physics Project on RLC Circuits*, GitHub, updated: 26 Feb. 2025. [Online]. Available: <https://github.com/A-n-d-R-o/Advanced-Higher-Physics-Project-on-RLC-Circuits>
- [3] T. Duncan, *Success in Electronics*, 1st ed. London: John Murray, 1983.
- [4] P. Burnett, *Advanced Higher Physics Theory*. MathsGroundWork, Oct. 2018.
- [5] Boundless, *20.5: RC Circuits*, Physics LibreTexts, accessed: 12 Feb. 2025. [Online]. Available: [https://phys.libretexts.org/Bookshelves/University_Physics/Physics_\(Boundless\)/20%3A_Circuits_and_Direct_Currents/20.5%3A_RC_Circuits](https://phys.libretexts.org/Bookshelves/University_Physics/Physics_(Boundless)/20%3A_Circuits_and_Direct_Currents/20.5%3A_RC_Circuits)
- [6] EEPower, *Series RC Circuit Analysis*, accessed: 12 Feb. 2025. [Online]. Available: <https://eepower.com/technical-articles/series-rc-circuit-analysis>
- [7] T. H. Glisson, *Introduction to Circuit Analysis and Design*. Springer, 2011.
- [8] pcprogrammer, *EEVblog Electronics Community Forum*, EEVblog, accessed: 12 Feb. 2025. [Online]. Available: <https://www.eevblog.com/forum/testgear/hantek-dso2xxx-schematics/>
- [9] B. Crowell, *4.3: Resonance*, Physics LibreTexts, accessed: 15 Feb. 2025. [Online]. Available: [https://phys.libretexts.org/Bookshelves/Conceptual_Physics/Conceptual_Physics_\(Crowell\)/04%3A_Conservation_of_Momentum/4.03%3A_Resonance](https://phys.libretexts.org/Bookshelves/Conceptual_Physics/Conceptual_Physics_(Crowell)/04%3A_Conservation_of_Momentum/4.03%3A_Resonance)

- [10] *RLC Series AC Circuits*, Lumen Learning, accessed: 15 Feb. 2025. [Online]. Available: <https://courses.lumenlearning.com/suny-physics/chapter/23-12-rlc-series-ac-circuits>
- [11] U. A. Bakshi and A. V. Bakshi, *Circuit Theory*, 1st ed. Pune: Technical Publications, 2009.
- [12] *Series RLC Circuit Analysis*, Basic Electronics Tutorials, accessed: 15 Feb. 2025. [Online]. Available: <https://www.electronics-tutorials.ws/accircuits/series-circuit.html>
- [13] Y. J. F. Kpomahou, C. Midiwanou, R. G. Agbokpanzo, L. A. Hinvi, and D. K. K. Adjaï, “Nonlinear resonances analysis of a rlc series circuit modeled by a modified van der pol oscillator,” 2018.
- [14] *Experiment 5: Transients and Oscillations in RLC Circuit*, University of Illinois at Urbana-Champaign, accessed: 15 Feb. 2025. [Online]. Available: https://courses.physics.illinois.edu/phys401/sp2010/Files/RLC/E5_Spring08.pdf
- [15] *Floating Measurements: Selection Guide*, Tektronix, accessed: 15 Feb. 2025. [Online]. Available: <https://www.tek.com/en/datasheet/floating-measurements-selection-guide>